MinBaS II

Mineral•Ballast• Sten **Område 1** **Rapport nr 1.5.3:03**

MinBaS II Område 1. Produktion och processutveckling
Delområde 1.5 Mineralteknik
Projekt 1.5.3 Bildanalys- Fragmentation Measurement of Bulk Material on Conveyor using 3D Vision

Slutrapport Steg 2

Fragmentation Measurement of Bulk Material on Conveyor using 3D Vision

Matthew Thurley & Tobias Andersson

Luleå University of Technology, Computer Science and Electrical Engineering

Luleå 8 December 2010

Contents

Summary of Reports

Progress report 26 January 2009[1]

Progress report 30 March 2009[2]

Progress report 27 May 2009[3]

Final report stage 1, Report number 1.5.3:01, 26 July 2009[4]

Progress report 10 December 2009[5]

Addendum to stage 1 final report and stage 2 application, Report number 1.5.3:02, 15 January 2010[6]

Progress report 24 May 2010 [7]

Progress report 2 September 2010[8]

Final Report stage 2, Report number 1.5.3:03, 8 December 2010 (this report)

Additional Attachments

The following additional attachments are appended to this report.

1. Paper providing detailed research results entitled *Online Product Identification during Ship Loading of Limestone based on Machine Vision* (Anderson et. al. 2010a)
2. Paper providing detailed research results entitled *A Machine Vision System for Estimation of Size Distributions by Weight of Limestone Particles during Ship Loading* (Anderson et. al. 2010b)

[1] Filename: MINBAS_II_ProgressReport_Project_1_5_3_BildAnalysisFragmenteringmatning_090126.pdf

[2] Filename: MINBAS_II_ProgressReport_Project_1_5_3_BildAnalysisFragmenteringmatning_090330.pdf

[3] Filename: MINBAS_II_ProgressReport_Project_1_5_3_BildAnalysisFragmenteringmatning_090527_merged.pdf

[4] Filename: MINBAS_II_FinalReport_Project_1.5.3_BildAnalysisFragmenteringmatning_090626-Etapp-1-merged.pdf

[5] Filename: MINBAS_II_ProgressReport_Project_1_5_3_BildAnalysisFragmenteringmatning_091210.pdf

[6] Filename: MINBAS_II_FinalReportAddendum_Project_1.5.3_BildAnalysisFragmenteringsmatning_100115-Ansokan.pdf

[7] Filename: MINBAS_II_ProgressReport_Project_1_5_3_BildAnalysisFragmenteringmatning_Stage2_100524.pdf

[8] Filename: MINBAS_II_ProgressReport_Project_1_5_3_BildAnalysisFragmenteringmatning_Stage2_100902.pdf

Sammanfattning

Projektet har levererat det utlovade proof-of-concept-systemet för automatiserad online-mätning.

Under fas 1 demonstrerades att det installerade systemet visar på en trend i rätt riktning vid observation av förändringar av materialstorlek (Thurley 2010).

Under fas 2 har en grundlig undersökning av tekniker för förbättring av uppskattningen av produktstorleksdistributionen gjorts, vilket gett följande intressanta resultat:

- Givet en uppsättning produkter i intervallen 20-40, 40-70 och 60-90mm har en klassificeringsstrategi, vilken säkerställer 98.8% korrekt prediktion av lastad produkt var 30:de sekund, utvecklats och validerats grundligt. (Andersson et. al. 2010a)
- Vidare har en detaljerad undersökning av optimeringen och estimeringsprocessen för siktningsstorlek gjorts, vilket har visat på nyckelproblem och genererat lovande resultat (Andersson et. al. 2010b)

En av de främsta komplikationerna i arbetet på Nordkalk är att de olika produkterna ibland uppvisar mycket olika genomsnittliga vikter per partikel inom lika storleksklasser. Eftersom ett maskinvisionssystem mäter partikelstorlek och beräknar antalet partiklar efter siktstorleksklass medan siktning används för att beräkna en totalvikt efter siktstorleksklass, är det nödvändigt att utföra en omvandling till vikt med hjälp av kunskap om partiklars medelvikt beroende av siktstorleksklass. Då sten tillhörande olika produkter har olika vikt trots att de är av samma storleksklass, blir hanteringen av denna process mer komplicerad och detta bidrar till ett fel i viktomvandlingen. Publicerade resultat (Andersson et. al. 2010b) uppvisar kapacitet att utföra denna viktomvandling, men det förutsätter förmågan att detektera vilken produkt som lastas samt kunskap om genomsnittsvikten för sten för varje siktstorleksklass. Denna typ av information om vikt skulle kunna insamlas rutinmässigt som en del av standardprocessen för siktning genom att dessutom räkna antalet stenar i varje viktklass.
Fördelen med forskningen inom produktidentifiering (Andersson et. al. 2010a) är att den kan uppnå precis vad Nordkalk behöver, mycket exakt produktidentifiering under lastning, och kräver ingen kunskap om vikten för individuella produkter. Med ytterligare arbete skulle ett sådant system även kunna göras självlärande och adaptivt för nya produkter med användning av samma typ av klassifikationsstrategi.

Summary

The project has delivered the promised proof-of-concept automated online measurement system.

During phase 1 the installed system was demonstrated to trend in the right direction tracking changes in the material size. (Thurley 2010)

During phase 2, in-depth investigation into techniques for improving the estimation of the product size distribution has been performed with interesting results as follows;

- Given a set of products in the ranges 20-40, 40-70, and 60-90mm, a classification strategy was developed and robustly validated that ensures 98.8% accurate prediction of the product being loaded every 30 seconds. (Andersson et. al. 2010a)
- Furthermore a detailed investigation of the optimization and sieve-size estimation process was performed illustrating key problems and generating promising results. (Andersson et. al. 2010b)

One of the key complications in the work at Nordkalk is that the different products sometimes exhibit very different average weights per particle at equal size classes. As a machine vision system sizes particles and calculates a number of particles by sieve-size-class, and sieving is used to calculate a total weight by sieve-size-

class, it is necessary to perform a weight transformation using knowledge of average particle weight by sieve-size-class. When rocks of different products have different weights even though they are the same sieve-size-class, this process becomes more complicated to handle and this contributes to a weight transformation error. Published results (Andersson et. al. 2010b) indicate the capability to perform this transformation but it requires the ability to detect which product is being loaded and knowledge of the average weight of rocks from each sieve-size-class. This kind of weight information could be collected on a routine basis as part of the standard sieving processes by additionally counting the number of rocks in each size class.

The advantage of the product identification research (Andersson et. al. 2010a) is that it can achieve exactly what Nordkalk needs, highly accurate product identification during loading, and requires no knowledge of the weight of individual products. With additional work, such a system could also be self-learning and adaptive to new products using the same kind of classification strategy.

Project Results

This stage 2 project continues the work on fragmentation measurement of bulk material on conveyor using 3D vision. The goal of this phase is improved accuracy, specifically to be able to better identify what size of material is being loaded to the ship.

In the 24th of May report,
MINBAS_II_ProgressReport_Project_1_5_3_BildAnalysisFragmenteringmatning_Stage2_100524.doc several goals for improving accuracy were outlined as follows;

1. Improve accuracy of online measurements between products in the 10-120mm range
2. Gain an understanding of how the technology can be applied to blasted material or material from a crusher
3. Understand how the average fragment weight at a given sieve size can change depending on which product the material is from
4. Generally improve the accuracy of size distribution estimation

Goals 1,3 and 4 are achieved in that accuracy is improved within the ranges 10-90mm (larger material has not been accessed) and is detailed in Andersson et. al. 2010b which is appended to this report. Goal 3 was also explained in detail in the progress report from the 24th of May 2010.

In evaluating goal 2 we consider how the technology would work in application to a crusher. There are two items worth considering here, first the presence of fines, and secondly the possibility of a varying range of material products exactly as we have experienced at Nordkalk. Less variation in material size, and a more continuous distribution of material (not the pre-sieved material as at Nordkalk) would likely make the imaging task simpler. Detection of areas of fines in the visible data was successfully demonstrated in an earlier project (Thurley, 2009) between LTU and LKAB. Further work is required before this capability would be ready for a robust prototype installation but preliminary results indicate the validity of the approach.

Future work

1. Build a consortium to perform a fragmentation measurement project for the purpose of crusher optimsation and control, and feedback to blasting. Sandvik is interested in this proposal and discussions are ongoing with Boliden, LKAB, Magnus Evertsson, Finn Ouchterlony, and the Sustainable Minerals Institute at the University of Queensland in Australia. A concrete proposal should be ready March/April 2011.
2. Discuss integration of the system at Nordkalk so that the results are available to the control room and they can be acted upon. Build a project to achieve this integration and the flexibility to handle future product changes .
3. Further research questions include;
    a. Investigation of particle particle shape to provide information on size and/or particle volume or weight.
    b. Robust validation of fines detection algorithms
    c. Computational improves and hardware implementations to achieve fast analysis (in the order of a few seconds) suitable for crusher control

References

Andersson, T, **Thurley, M** & **Carlson, JE** 2010a, **'On-line product identification during ship loading of limestone based on machine vision'**, *Machine Vision & Applications.*

Andersson, T, **Thurley, M** & **Carlson, JE** 2010b, **'A machine vision system for estimation of size distributions by weight of limestone particles during ship loading'**, *Minerals Engineering.*

Thurley, M 2009, **'Fragmentation size measurement in LHD buckets using 3D surface imaging'**, In *Fragblast 9: Rock Fragmentation By Blasting. Proceedings of the 9th International Symposium On Rock Fragmentation By Blasting,* CRC Press.

Thurley, M 2010, **'Automated online measurement of limestone particle size distributions using 3D range data'**, *Journal of Process Control.*

Paper F

On-line Product Identification during Ship Loading of Limestone based on Machine Vision

Authors:
Tobias Andersson, Matthew J. Thurley and Johan E. Carlson

Reformatted version of paper submitted to:
Machine Vision and Applications, 2010

On-line Product Identification during Ship Loading of Limestone based on Machine Vision

Tobias Andersson, Matthew J. Thurley and Johan E. Carlson

Abstract

In the aggregates and mining industries suppliers of particulate material, such as crushed rock and pelletised iron ore, produce material where the particle size is a key differentiating factor in the quality of the material. Material is classified by size using sieving or screening to produce various products, such as crushed limestone in the sieve-size range 20 - 40 mm. Quality control of particulate material size in industry is usually performed by manual sampling and sieving techniques. These techniques are typically infrequent and have long response times making them unsuitable for online quality control even during the loading of ships. Automatic on-line analysis of rock size based on image analysis techniques would allow non-invasive, frequent and consistent measurement that enables on-line product identification, and prevent loading, shipping and delivery of the wrong sized product. In this research, we present classification algorithms based on nominal logistic regression and discriminant analysis to automatically identify products being loaded onto ships. A measurement campaign has been conducted during three days of normal production when three different products were loaded onto ships. The size ranges for the majority of rocks being loaded onto the ships were 20 - 40 mm, 40 - 70 mm and 60 - 90 mm for the three products. Half an hour of production data for each product was used to train the classifiers. Validation of both classifiers' performance shows that the overall accuracy was 98.8 %. We conclude that on-line automatic product identification is achieved using classifiers based on both nominal logistic regression and discriminant analysis.

1 Introduction

In the aggregates and mining industries suppliers of particulate material, such as crushed rock and pelletised iron ore, produce material where the particle size is a key differentiating factor in the quality of the material. Material is classified by size using sieving or screening to produce various products, such as crushed limestone in the sieve-size range 20 - 40 mm. The final products are stored at different locations at the production area until they are loaded onto ships and delivered to buyers. During the loading of ships operators at the plant direct personnel to load material of a specific product onto a conveyor belt that transport the rocks to the ships.

Suppliers are paid to deliver rocks of particular sizes that buyers can use. For quality control, manual sampling and sieving of rocks that are loaded is conducted. Manual

sampling and sieving techniques are the industry standard, and the size distribution of particles is presented as a cumulative percentage by weight for different size classes. However, as the manual sampling is performed infrequently and is time-consuming, there are long response times before an estimate of the sieve-size distribution is available for operators at a quarry. The response times can be as long as 12-48 hours from when a sample is taken for sieve-size analysis until the result is measured in the laboratory. During this time the loading of ships is finished and the result from sieve-size analysis is only useful for quality control and monitoring of what has been shipped. Sampling, sieving, and material handling times coupled with delays between steps make manual sampling and sieving unsuitable for efficient control of the loading of ships. During loading, operators have to assume that the products have been correctly produced and organized accordingly in the production area.

Image analysis techniques promise a non-invasive, frequent and consistent solution to determining the size distribution of particles in a pile and would be suitable for on-line product identification, and prevent loading, shipping and delivery of the wrong sized product. Such techniques capture information about the surface of the pile that is then used to infer the particle size distribution.

However, the implementation of an imaging system that is accurate and robust is not a trivial and quick process. Assuming a robust and accurate surface data capturing system with insignificant error, there are a number of sources of error relevant to surface analysis techniques that need consideration and investigation. It may be tempting to use multivariate calibration techniques to transfer surface data to known sieve-size distributions, however, it is important to consider the following sources of error and minimise them separately to get a general solution that is known to be robust to all errors:

- Segregation and grouping error, more generally known as the Brazil nut effect [1], describes the tendency of the pile to separate into groups of similarly sized particles. It is caused by vibration or motion (for example. as rocks are transported by truck or conveyor), with large particles being moved to the surface.

- Capturing error [2],[3, Chap. 4] describes the varying probability based on size that a particle will appear on the surface of the pile.

- Profile error describes the fact that only one side of an entirely visible particle can be seen, which may bias the estimate of particle size.

- Overlapped particle error [4] describes the fact that many particles are only partially visible, and a large bias to the smaller size classes results if they are treated as small, entirely visible particles and sized using only their visible profile.

- Weight transformation error describes the fact that the weight of particles in a specific sieve-size class may vary significantly. As a sieve-size class is defined by its upper and lower bound where particles fall though, elongated particles may have significantly larger volumes than other particles.

The main aim of this research is develop techniques for quality control where the size distribution based on weight has limited importance. Thus, the surface analysis does not need to estimate the size distribution and weight transformation error is ignored in study. Segregation and capturing errors are present in our data but for an application that needs to discriminate among different products, these errors can be ignored. We have previously shown that visibility classification can overcome the overlapped particle error [5, 6]. In short, it is critical to identify and exclude any partially visible particles before any size estimates of particles in piles are made. This is possible with classification algorithms that use a 3D visibility measure proposed by Thurley and Ng [4]. In the presented study, we eliminate overlapped particle error by classification using this 3D visibility measure. And finally, profile error is considered to not be significant when using the best-fit rectangle [7] to estimate the size of non-overlapped particles.

Limited work has been published on product identification of particulate material. More work has been presented on size and shape analysis of rock fragments using imaging with the aim of estimating sieve-size distributions, and we extend our literature review to include work presented in that field. Particle size measurement using imaging has been the subject of research and development for over 25 years [8] with a legacy of predominantly photographic based systems with widely varying degrees of success and no general solution available on the market. Photographic based 2D imaging systems are subject to bias due to uneven lighting conditions, excessive shadowing, color and texture variation in the material, and lack of distinction between overlapped and non-overlapped fragments. In their review of a commercial photographic based 2D system Potts and Ouchterlony [9, pg. vi, viii] report that for their application the system erroneously assumes the resultant size distribution is unimodal and they conclude by expressing strong reservations saying 2D 'imaging has a certain but limited usefulness when measuring the fragment size distribution in a muckpile or from a belt in an accurate way. It could probably detect rough tendencies in fragmentation variations, if the lighting conditions do not vary too much, and if cover glasses for camera lenses are kept clean'. 3D imaging allows measurements of the surface of piles with height information that may be used to achieve robust and accurate analysis. The only work that has been presented using 3D imaging that performs automated on-line analysis of rock fragments transported on conveyor belts are based on active laser triangulation [10] and stereo imaging [11].

In this paper, classifiers were trained to discriminate among different products being loaded onto ships via conveyor belt systems. Samples were collected during three days of normal production at a limestone quarry when three different products were loaded onto ships. The size range for the majority of rocks being loaded was 20 - 40, 40 - 70 and 60 - 90 mm for the three products. Half an hour of production data for each product was used to train classifiers that were based on discriminant analysis and nominal logistic regression. We note that this research does not relate to the choice of classification method. It is however interesting to present classifiers based on both methods as they are widely used in practice. The classifiers were trained and validated using the hold out method [12, Ch. 7].

The paper is organized as follows. In section 2, a background to this research is

given summarizing the measurement system used and required analysis of collected data that result in size information of samples that is used in this research. In section 3, theory of how size estimates of rocks is used to form features used in the classification is given. Descriptions of classification methods are also presented in section 3. The measurement campaign conducted during three days of production to collect data is detailed in section 4.1. Analysis of training data, training of classifiers and validation of classifiers' performance is given in section 4.2 to 4.4. Finally, the conclusions are presented in section 5.

2 Research background

We [13] have previously implemented an industrial prototype that measures the pellet sieve-size distribution among nine sieve-size classes between 5 mm and 16+ mm. A 3D surface data capturing system based on active triangulation is used to collect the data. Segmentation of the data is achieved using algorithms based on mathematical morphology of 3D surface data. It was also shown that sizing of identified pellets gives promising results using the best-fit rectangle [7] measure.

The techniques have been further developed and implemented in an industrial prototype that measures the size distribution on limestone fragments on conveyor belts [10]. We refer to previous publications for a more detailed discussion on how 3D surface data are analyzed. However, we will give a short description of the analysis in this section.

2.1 Hardware setup

We use an industrial measurement system based on active triangulation to capture 3D surface data of the flow of rock material on the conveyor belt. The system consists of a laser with line-generating optics and one camera mounted at an approximately 24-degree angle between the camera line of sight and the laser line. The laser and camera is built into a protective case as seen in figure 1, which is a photograph of the protective case viewed from below the conveyor belt. The system collects images extract the laser line, convert the images to 3D surface data and perform analysis of the captured 3D surface data.

Also, a pulse encoder is mounted to the conveyor belt to allow synchronization of the camera to take 3D profiles of the laser line for every 1 mm movement of the conveyor belt. The data captured with this technique are highly accurate and provides high density 3D point data. A close-up of the captured 3D data is seen in Fig. 2(a). The computational speed of the collection of data, conversion to 3D surface data and analysis of data allows samples to be taken at intervals of approximately 30 seconds.

2.2 Segmentation of 3D Range Data

The first step of the analysis of the 3D surface data is to identify the individual rock fragments. Thurley [10] developed a technique to segment 3D range data to identify

Figure 1: View of laser generating optics and camera mounted into a protective case. Photograph is taken from below the conveyor belt.

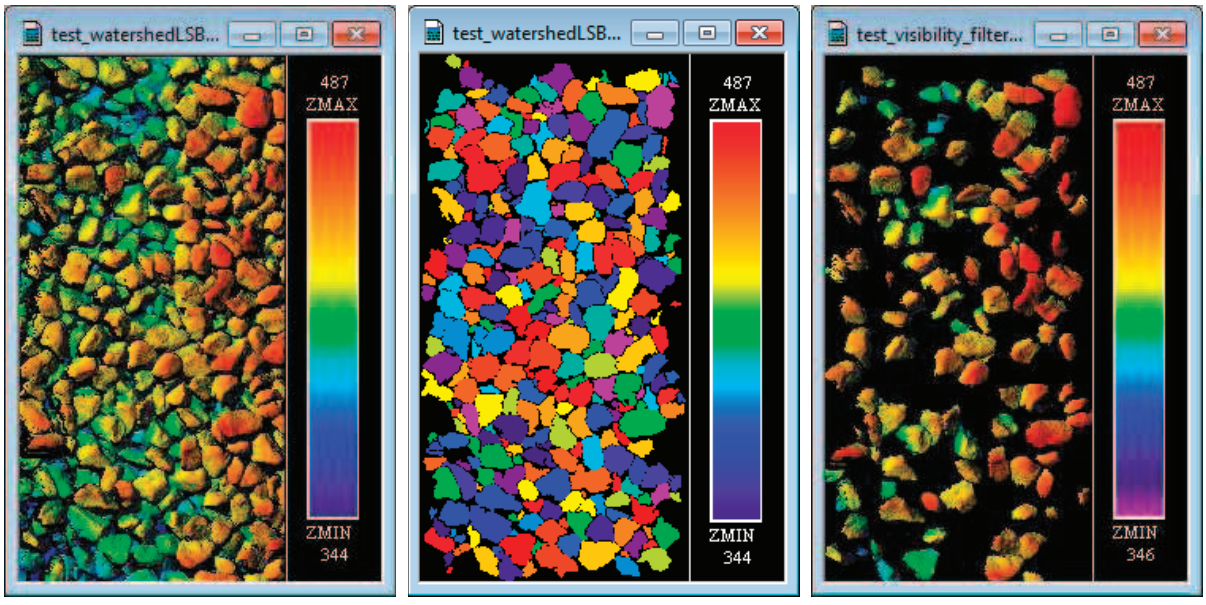

(a) 3D surface data (b) Segmentation (c) Non-overlapped

Figure 2: Collected 3D surface data (a), segmentation (b) and identification of non-overlapped particles (c).

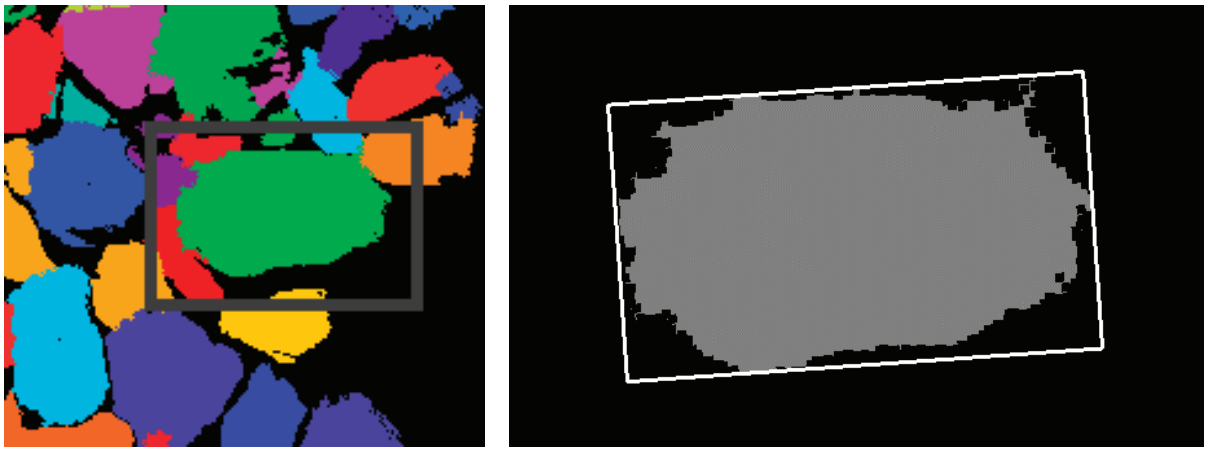

(a) Identified non-overlapped rock (b) Calkulated best-fit rectangle

Figure 3: Identified non-overlapped rock (a) and calculated best-fit rectangle (b).

rock fragments by a series of operations predominantly based on morphological image processing. The technique detects edges that are used to facilitate seed formation for the watershed segmentation algorithm [14, watershed transform]. Fig. 2(b) shows the segmentation result.

2.3 Overcoming Overlapped Particle Error

In order to minimize the overlapped particle error, it is critical to identify and exclude any partially visible particles from the analysis before size estimates are made. Using an automatic measure of the visibility of rocks [10, 4], overlapped particles are identified and excluded from any further analysis. In Fig. 2(c) overlapped particles are identified and removed from previous figures.

2.4 Sizing

For each non-overlapped rock, the measure best-fit rectangle [7] is calculated. The best-fit rectangle is the rectangle of minimum area that fits around the 2D projection of each region. The 3D surface data contain X-, Y- and Z-data where the Z-data contain height information. The height information is not used to calculate the best-fit rectangle measure. In Fig. 3(a) a close up of all regions is shown. The regions enclosed by the white rectangle is determined to be a non-overlapped rock and therefore valid for size estimation. The 2D projection of the region and the calculated best-fit rectangle is shown in Fig. 3(b).

Each non-overlapping rock in a sample may be determined to belong to a specific sieve-size class based on the calculated area of the best-fit rectangle measure. By determining what sieve-size class each rock in a sample belongs to a sieve-size distribution by number of rocks can be estimated for the surface of a pile.

2.5 Weight transformation

If an imaging system is going to report a sieve-size distribution following the industrial standard, then the system needs to be able to transform number of rocks to weight of rocks. Weight transformation may be found by collecting manual sieving results and counting the number of particles in each size class in order to determine an average weight of a fragment by size class. This transformation is still a source of error when estimating the sieve-size distribution based on weight of rocks as we have found deviation in the average weight of fragments of similar sieve-size classes [10]. We note that the size distribution does not need to be estimated for the purpose of product identification. Thus, weight transformation to estimate the sieve-size distribution based on weight is not used in this research.

3 Theory

As product identification may be implemented based only on the size estimates of non-overlapped particles we detail how the size estimates are used to describe products in this section. We also outline the classification methods used in this research and discuss how to validate the classifier's performance.

3.1 Sizing

For each sample collected by the imaging system, the non-overlapped rocks are identified and their size are estimated by calculating the area of the best-fit rectangle. The estimated size for all non-overlapped rocks in a sample is representative of the rocks on the surface of the pile. The distribution of the estimated sizes is then used to discriminate among different products of rocks.

The distribution of best-fit rectangle values for each sample is summarized by the median and inter-quartile range (IQR) [15]. The median and IQR are robust measures that are not sensitive to outliers and describe the middle value and spread of a distribution. The descriptive features median and IQR will be used to train classifiers to discriminate among different products.

In figure 4, distributions of the best-fit rectangle area values for two samples representing the products 20–40 and 40–70 mm are shown. The median is depicted with a vertical line in figures and the IQR is depicted as the range around the median. We can note that the distribution is skewed to lower values for both products. There are a few rocks in the samples that are significantly larger than the majority of rocks but the median value is not affected much by best-fit rectangle values of these rocks. For the product with smaller rocks, 20–40 mm, the median value is 1260 mm^2. The median for the product with larger rocks, 40–70 mm, is larger with a value of 3440 mm^2.

It is also clear in the figures that the IQR is larger for the 40–70 mm product. For the 20–40 mm product the IQR is 1014 mm^2 (between 782 and 1796 mm^2) and for the 40–70 mm product the IQR is 3361 mm^2 (between 2249 and 5610 mm^2). The difference of

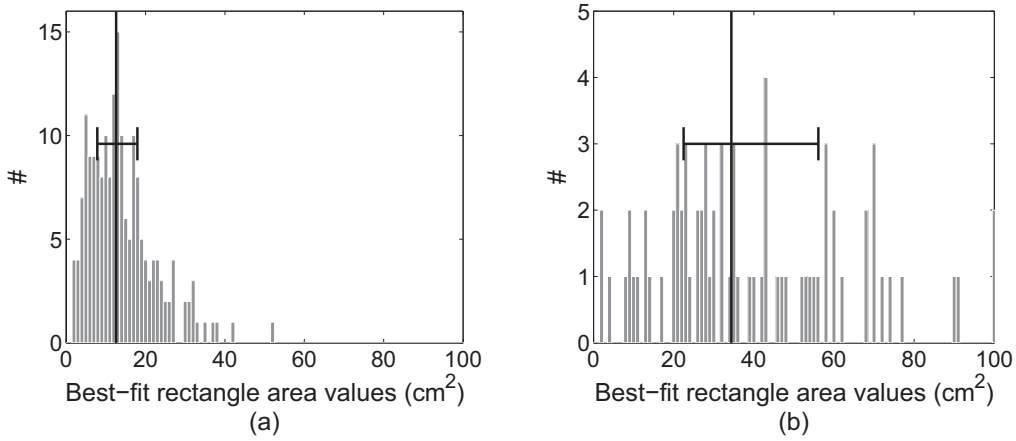

Figure 4: Distribution of best-fit rectangle area values for the products "20–40" (a) and "40–70" mm (b).

the IQR for the two products may partially be explained by the fact that the majority of rocks in the 20–40 and 40–70 mm products should range between sieve-sizes 20 to 40 mm and 40 to 70 mm, which are ranges of 20 and 30 mm respectively. Thus, the IQR should be larger for the product composed of rocks that belong to a larger range of sieve-size classes.

3.2 Classification

In general, classifiers predict a *response* from a set of *feature values*. For product identification, the response is the predicted product category given a set of feature values that describe a sample. Features that discriminate among products are the median and the IQR of the estimated size of rocks in a sample. More information on classification can be found in the following books: [16] and [12].

Classifiers can be implemented based on different methods. Common statistical methods include discriminant analysis and logistic regression. The choice of classification method may affect the overall classification accuracy, depending on the distribution of the feature values. However, this research does not relate to the choice of classification method for the highest classification accuracy and only notes that the distribution of feature values in a data set may be important in order to choose a proper classification method. The choice of which of discriminant analysis and logistic regression to use has previously been studied [17], usually selecting one of the two methods. The theory for discriminant analysis is based on feature values that belong to a multivariate normal distribution, and complete equality of the populations' covariance matrices. The first criterion is rarely fulfilled in practice but can sometimes be enforced by some variable transformation. The assumption of equal covariance matrices is, however, typically not

valid. Evaluating the performance of discriminant analysis is still relevant because of its computational simplicity compared to logistic regression. For logistic regression, there is no assumption that feature values belong to a multivariate normal distribution.

We used MATLAB®to perform all analysis in this research. Also, the function *mnrfit* in the Statistics Toolbox™was used to train the nominal logistic regression model.

Nominal Logistic Regression

Logistic regression is a statistical classification method that can be used when the response variables are binary, ordinal or nominal. When the response variable is a set of categories without natural order and consists of more than two categories, *nominal* logistic regression should be used [12].

The basic idea with logistic regression is to estimate the probability $\hat{p}_j$ of a measurement point belonging to each category j. Basically, for three categories, three probabilities are estimated and the category with highest probability is chosen. The probabilities, $\hat{p}_0, \hat{p}_1, ..., \hat{p}_{J-1}$, where J is the number of categories, are estimated using the vector of estimated model parameters $\mathbf{x}$ and the estimated regression coefficients $\beta_j, ..., \beta_{J-1}$. When there are more than two categories, one of them is chosen as the comparison category, hence only $J-1$ regression coefficient vectors are required.

The form of the nominal logistic regression model is shown in Eqs. 1 and 2, where y is the response variable, $\mathbf{x}$ is a feature vector, β_j are parameters that depend on j. To clarify, y is the response variable that the classifier predicts. In our case, the product being transported on a conveyor belt. The classifier predicted the product being loaded based on the feature values in feature vector $\mathbf{x}$, which was composed of measures of the distribution of best-fit rectangle values. The classifier was trained to classify correctly by fitting the model, or more specifically, the parameters in β_j, via the use of maximum likelihood estimation to a training set with known response values and feature values.

$$\hat{p}_0 = P(y = 0|\mathbf{x}) = \frac{1}{1 + \sum_{j=1}^{J-1} \mathrm{e}^{\beta_j^T [1,\mathbf{x}]}} \tag{1}$$

$$\hat{p}_i = P(y = i|\mathbf{x}) = \frac{\mathrm{e}^{\beta_i^T [1,\mathbf{x}]}}{1 + \sum_{j=1}^{J-1} \mathrm{e}^{\beta_j^T [1,\mathbf{x}]}} \qquad \text{for } i = 2, ..., J \tag{2}$$

Eqs. 1 and 2 are used to calculate the estimated probability $\hat{p}_i$ of a new sample belonging to a category $i = 0, 1, ..., J-1$ where J is the number of possible response values. The response of the classifier for a sample is the category with highest predicted probability. That is, the responses of the classifiers are $y = k$ where $p_k > p_l$ for all $l \neq k$.

Discriminant Analysis

The basic idea with discriminant analysis is to estimate the distances from a sample to a number of predefined reference categories and classify the sample to the closest category. The actual distance metric has a wide range of appearances [12], and in this study a quadratic distance metric seen in equation 3 is used. In a quadratic discriminant rule, the minimum squared distance from the estimated parameters at a new measurement point to each reference category is calculated. The response of the classifiers are $y = k$ where $\hat{d}_k < \hat{d}_j$ for all $j \neq k$.

The quadratic distance from a point to the reference categories is calculated by Eq. 3, for the categories $i = 0, 1, ..., J-1$ where J is the number of possible response values. The parameters $\hat{\boldsymbol{\mu}}_j$ and $\hat{\mathbf{C}}_j$ are estimated by assuming that each reference category have a multivariate normal distribution, i.e $\mathbf{x}_j \sim N(\boldsymbol{\mu}_j, \mathbf{C}_j)$, where $\mathbf{x}_j$ is the vector of feature values belonging to category j.

$$\hat{d}_j = \frac{1}{2}(\mathbf{x} - \hat{\boldsymbol{\mu}}_j)^T \hat{\mathbf{C}}_j^{-1}(\mathbf{x} - \hat{\boldsymbol{\mu}}_j) + \frac{1}{2}\log_{10}|\hat{\mathbf{C}}_j^{-1}| + \log_{10}(r_j) \tag{3}$$

3.3 Validation

The purpose of validation of classifier performance is to get an estimate of how well classifiers discriminate among classes. Three different validation methods are outlined below:

- The *resubstitution method* estimates the classifier performance on the same data that were used to train the classifier. It has to be emphasized that the use of resubstitution to estimate a classifier's performance will generate overoptimistic results. Hence, the resubstitution method is not recommended.

- The *holdout method* is a technique where the classifier is developed on a specific training set. A test set (or validation set), separate from the training set, is used to estimate how the classifier performs on new data. The test set is held out during all analysis and design of the classifier. This limit the bias that the resubstitution method has and this method gives an unbiased estimate of the classifier's performance. It has to be mentioned that using the holdout method might result in a classification rule that is not the best possible as all available data is not used to train the classifier.

- The *cross-validation method* estimates classifiers performance by dividing the data into k blocks. The classifier's performance is estimated by holding out one block at a time, training the classifier using the available $k-1$ blocks and estimating the classifier's performance on the held out fold. This procedure is performed so that all k blocks are used as the test set once. In each iteration during the cross-validation, the classifiers decision boundaries will vary slightly from a classifier that is built on all available data. But most importantly, the classifier is evaluated on data that has not been part of the training set, which results in an unbiased estimate of the

Table 1: Loading scheme of ships during the measurement campaign spanning over 3 days.

Day	Loading time	Product (mm)	Manual samples	Imaging samples
1	07:00 - 16:00	60–90	4	345
1	17:00 - 19:00	40–70	2	174
2	07:00 - 15:00	40–70	5	561
3	08:00 - 15:00	20–40	4	469

classifier's performance. This method is particularly useful when the amount of available data is small.

How well the classifiers performed in this research was validated using the holdout method. We use the holdout method since the number of samples available for training the classifiers in a practical situation might be half an hour of production data, which corresponds to approximately 60 samples. As our data consisted of data collected during normal production when three different products were loaded, we used the 60 first samples acquired with the imaging system for each product to create the training set. All remaining samples were used for validation.

4 Measurement results

4.1 Measurement campaign

A measurement campaign was conducted at Nordkalk's limestone quarry in Storugns during three days when two ships were loaded with three different products. Typically, one ship is loaded with one product. During the measurement campaign one larger ship was loaded with two different products, specifically 40–70 and 60–90 mm. In addition, a smaller ship was loaded with the product 20–40 mm. The loading of rocks began on day 1 with the product 60–90 mm and at 15:22 the product being loaded were changed to 40–70 mm. During day 2 only 40–70 mm were loaded and the first ship departed. The smaller ship was loaded with the product 20–40 mm during day 3. The loading scheme is summarized in Table 1.

The conveyor belt that transports rocks to ships is equipped with a balance to monitor the amount of rocks that have been loaded. During normal production this is used to synchronize an automatic sampling machine to collect 3 manual samples for every product being loaded. The manual samples are later analyzed in the laboratory to produce sieve-size distributions and chemical analysis of the material. During the measurement campaign we used the cumulative weight of rocks being loaded onto the ships to collect manual samples of rocks that where loaded onto ships every 1000 tons. This resulted in 4, 7 and 4 manual samples of the 20–40, 40–70 and 60–90 mm products respectively. At the same time, the measurement system based on image analysis collected and analyzed 469, 735 and 345 samples.

The samples collected with the imaging system were divided into two sets of data. The first set is the *training set* and is used for graphical examination and training of classifiers. The training set is composed of the first 60 samples for each product. The second set is the *validation set* and is held out during graphical examination and training of classifiers. The validation set is used to estimate the classifier performance and is composed of remaining samples collected by the imaging system during loading of the ships.

4.2 Graphical examination of descriptive data

Graphical examination of the descriptive features provides information about how features are related and may also indicate if features are multivariate normally distributed. This information is important when considering the use of discriminant analysis as this assumes that the features are multivariate normally distributed. We note that even if the features violate this assumption, discriminant analysis may still produce practically useful classification results.

In Figure 5 the descriptive features for samples in the training set are depicted using scatter plots. Feature values from the three different categories are depicted with square-, circle- and diamond-shapes to clarify the discriminant ability of the features. It is clear that the three products are completely separated. That is, it is possible to divide the feature space into regions that completely separates points belonging to one category from other categories. We note that the features appears to be multivariate normally distributed and both logistic regression and discriminant analyisis should be valid to use for classification.

4.3 Training of classifiers

The training set consists of the descriptive features, median and IQR, for the first 60 samples of the three products. The two features of each sample in the training set represent one row in the feature matrix, $\mathbf{X}$. The known product for each sample is represented in the response variable y. In total, we have 180 training samples with two descriptive features with the ability to discriminate among three categories that are used to train the classifiers.

The classifier based on logistic regression was trained by fitting the model, or more specifically, the parameters in β_j in Eqs. 1 and 2, via the use of maximum likelihood estimation to the training set. Since we have three categories, the 60–90 mm product is chosen as the comparison category labelled $j = 0$. The 20–40 and 40–70 mm products are labelled $j = 1$ and 2 respectively. The classifier is composed of two parameter vectors seen in Table 2. The first vector is estimted using the calculated median and IQR for samples from category 1 and the reference category 0 (Logit 1, in table 2) and the second using the median and IQR for samples from category 2 and the reference category 0 (Logit 2, in table 2). The regression coefficients β_i and the corresponding standard error $\hat{\text{se}}_{\beta_i}$ are presented. Also given in the table are p-values for each parameter, for which a value less than 0.05 indicates that the coefficient cannot be excluded. A p-value less than

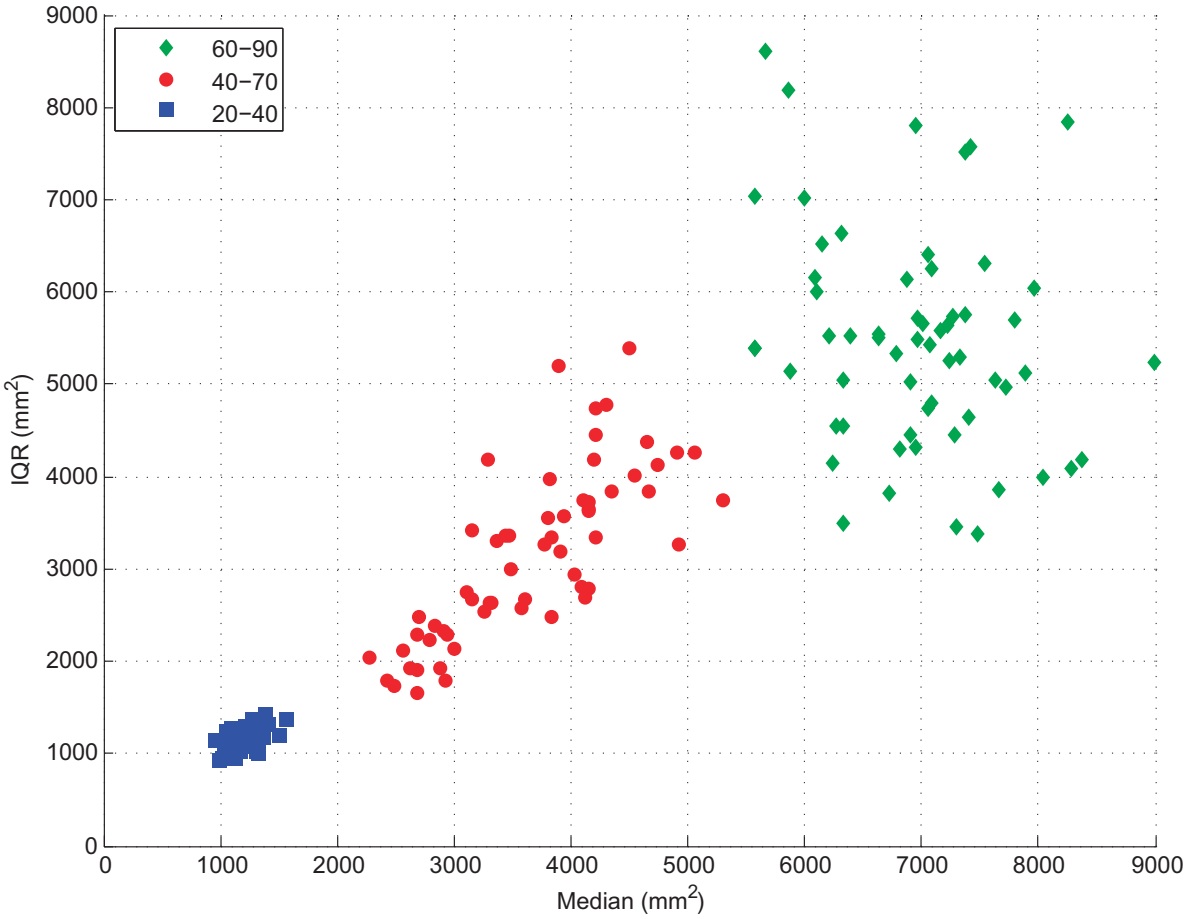

Figure 5: Scatter plot of the descriptive features median and IQR for samples in the training set. It is clear that the features are suitable for discrimination among products as the three products are completely separable.

0.05 indicates that we can reject the null hypothesis, which is that the parameter is not significant, when a significance level of 95 % is used. The p-value relating to IQR is 0.05 for the second parameter vector, which is on the limit for rejecting the null hypothesis. However, we conclude by previous graphical observations, see Fig. 4 and 5, and the values for $\hat{\beta}_2$, see $\hat{\text{se}}_{\beta_2}$ and p-value, that the coefficient relating to IQR is significant and cannot be excluded from the model.

Training the classifier based on discriminant analysis is basically estimating the means $\hat{\boldsymbol{\mu}}_j$ and covariance matrices $\hat{\mathbf{C}}_j$ for each category in the training data. The estimated parameters can be seen in Table 3, where the means $\hat{\boldsymbol{\mu}}_j$ for both median and IQR values clearly differ among the three categories. One can see that both the means $\hat{\boldsymbol{\mu}}_j$ of median and IQR increase as the categories represent larger sized products. The diagonal elements in the covariance matrices $\hat{\mathbf{C}}_j$ represent the variances of the median and IQR for each category. One can see that for the smallest product, when $j = 1$, the variances

Table 2: Properties of the classifier based on nominal logistic regression.

Predictor	$\hat{\beta}_i$	$\hat{\text{se}}_{\beta_i}$	p-value
Logit 1: (1/0)			
Constant	26.44	2.55	< 0.001
Median	-7.58	0.112	< 0.001
IQR	-0.0407	0.121	0.740
Logit 2: (2/0)			
Constant	18.21	2.35	< 0.001
Median	-0.271	0.0429	< 0.001
IQR	-0.0782	0.0399	0.050

Table 3: Properties of the classifier based on discriminant analysis.

			$\hat{\mathbf{C}}_j$	
Category	Feature	$\hat{\boldsymbol{\mu}}_j$	Median	IQR
$j = 1$				
	Median	1201.4	16150	7532
	IQR	1149.4	7532	12345
$j = 2$				
	Median	3659.0	561836	539457
	IQR	3152.5	539457	853550
$j = 0$				
	Median	6954.7	568310	-212423
	IQR	5471.5	-212423	1399767

(diagonal elements in the covariance matrix $\hat{\mathbf{C}}_1$) of the median and IQR are smaller in comparison with larger products. This means that the spread of the values is smaller for the smaller product, which also have been seen in Figure 5. One can also conclude that the assumption of equal covariance matrices is violated as $\hat{\mathbf{C}}_0$ clearly differs from $\hat{\mathbf{C}}_1$ and $\hat{\mathbf{C}}_2$.

4.4 Validation of classifiers performance

The classifiers' performance were validated on the data that was held out during graphical examination and training. This gives an unbiased estimate of how well the classifiers perform on new data. The number of samples in the validation set for each product is 409, 675 and 285 samples for the products 20–40, 40–70 and 60–90 mm respectively. These samples are classified with the trained classifiers and the overall classification accuracy is calculated from the number of misclassifications. Also, category-specific classifica-

Table 4: Confusion matrix that shows the category-specific classification accuracies of the classifier based on logistic regression. The figures in parentheses are the number of samples of a known product classified as a specific product.

	Predicted product		
Known product	20–40	40–70	60–90
20–40	**100**$^{(409)}$	0	0
40–70	0	**99.7**$^{(673)}$	0.3$^{(2)}$
60–90	0	5.3$^{(15)}$	**94.7**$^{(270)}$

Table 5: Confusion matrix that shows the category-specific classification accuracies of the classifier based on discriminant analysis. The figures in parentheses are the number of samples of a known product classified as a specific product.

	Predicted product		
Known product	20 - 40	40 - 70	60 - 90
20–40	**99.5**$^{(407)}$	0.5$^{(2)}$	0
40–70	0	**99.4**$^{(671)}$	0.6$^{(4)}$
60–90	0	3.9$^{(11)}$	**96.1**$^{(274)}$

tion accuracies will be presented to show how well the classifiers discriminate particular products. Finally, we present the estimated probabilities for the classifier based on nominal logistic regression for product identification during 3 days of production. Analyzing the estimated probabilities provides information on how confident the predictions of the classifier are.

The number of misclassified samples for both classifiers was 17 of a total number of 1369 samples. That is, the overall classification accuracy was approximately 98.8 %. We note that the overall classification accuracies indicate that both methods are useful for a practical implementation of product identification.

A more detailed analysis of the performance of the classifiers is shown in Tables 4 and 5 where category-specific classification accuracies are shown. We note that category-specific classification accuracies deviate slightly between the two classifiers. The classifier based on nominal logistic regression classifies all samples from the 20–40 mm product correctly. The classifier based on discriminant analysis misclassifies 2 samples of the 20–40 mm product as a 40–70 mm product. However, both classifiers have high classification accuracies for the product 20–40 mm and this is expected as the size range of the rocks in that product does not overlap any other product. As expected there are more misclassifications between the products 40–70 and 60–90 mm but the amount of misclassifications are still small when a practical implementation of product identification is considered.

The probabilities estimated by the classifier based on nominal logistic regression for

product identification during three days of production is shown in Figure 6. There are three training periods visible in the figure where each training period lasted for half an hour effective loading time. The first training period is at the beginning of day 1 when loading of the product 60–90 mm began. The 60–90 mm product continued to be loaded until 15:30 when loading changed to the 40–70 mm product and the second training period is seen. The third training period containing samples from the product 20–40 mm is seen in the beginning of day 3.

The estimated probabilities for the smallest product, 20–40 mm, loaded during day 3 are close to 1 for predictions that the samples belong to the product 20–40 mm, i.e. $\hat{p}_1 \approx 1$ for all samples. This means that the classifier makes a clear distinction between the correct product and the others. It is interesting to note that during day 1, when the product 60–90 mm is loaded, the estimated probabilities for the correct product are close to 1 for the majority of samples, i.e. $\hat{p}_0 \approx 1$. But there are samples where the estimated probability is closer to 0.5 and at the same time as the estimated probability for the sample to be product 40–70 mm is close to 0.5. These are samples where the rocks are closer to the lower bound of the allowed range for the 60–90 mm product.

Other interesting information can be seen by looking at the estimated probabilities for loading during day 2. During the entire day the classifier predicts the majority of samples correct but the estimated probabilities that the samples belong to any of the other two products indicate variation of rocks sizes during the loading process. Between 09:00 and 12:00 the estimated probability that the samples belong to the smaller product 20–40 are higher than the larger product 60–90. And between 12:30 and 13:20 the estimated probability that the samples belong to the larger product 60–90 are higher than the smaller product 20–40. Even though the products are identified correctly trends can be seen in this data.

Finally, we note that the validated accuracy for the classifiers based on both nominal logistic regression and discriminant analysis indicate that both classifiers can be used in a practical implementation. The accuracy is considered high and the estimated probabilities for classification follow expected trends.

5 Conclusions

We have shown how sizing results from an industrial prototype that captures the 3D surface of conveyor belts may be used to enable product identification. Data collected during a measurement campaign over three days of production when loading three different products onto ships was used in this research. Training data for classification algorithms were taken from the first half an hour of loading of each product. The remaining data collected during loading of ships was used to validate the classifiers performance. The most important findings were:

- The industrial prototype produce size estimates based on the best-fit rectangle area fitted to each non-overlapped rock in a sample. The measures median and IQR of

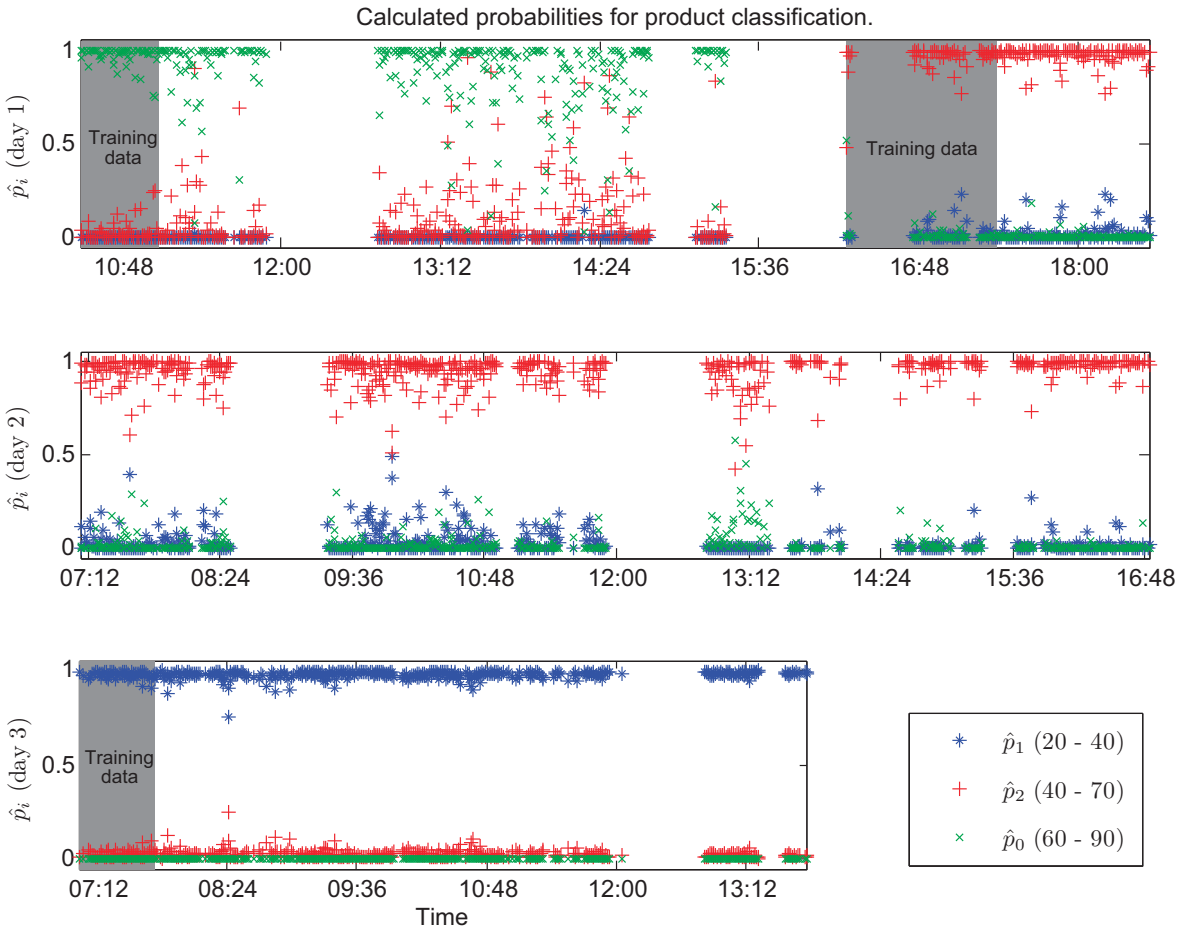

Figure 6: The result from the classification for three days of production.

the distribution of size estimates are suitable for product identification as complete separation among products is seen in the training data.

- Two classifiers were trained using half an hour of production data for each product. The classifiers were based on nominal logistic regression and discriminant analysis. Training classifiers using half an hour of production data is a practical time if this technique shall be used at other sites with other material. Also, limited training time is beneficial if new products are to be added to the system.

- Validation of the classifiers on data not used for training shows that both classification methods produce overall classification accuracies of 98.8 %. The category-specific classification accuracies are perfect for the product (20–40 mm) where the size of the majority of rocks do not overlap with other products when using nominal logistic regression but a few misclassifications occur when discriminant analysis is used. For products where the size of the majority of rocks slightly overlaps (40–70 mm and 60–90 mm), a few miss-classifications occur using both classification

methods. However, this is expected and might be correct as the distribution of size estimates for rocks in these products might overlap because of the actual properties of those samples.

- The classification accuracy combined with the limited sample size used for training the classifiers show that this technique is suitable for product identification. Once the classifier has been trained, the analysis produce quick, robust and accurate product identification that can be used to aid operators loading ships to track what actually is being loaded and stop loading when the product deviates out of the expected range.

6 Acknowledgments

We wish to thank ProcessIT Innovations for all their time and effort in making this research possible. We also want to thank MinBaS II Research program and Nordkalk for their participation and support. We especially say thank you to Madeleine Hägbom and Kajsa Hägbom for helping us with laboratory work at Nordkalk. Finally, we thank our measurement technology partners, MBV Systems. In addition we acknowledge the EU INTERREG IVA Nord program for partially supporting this research.

References

[1] A. Rosato, K. J. Strandburg, F. Prinz, and R. H. Swendsen, "Why the brazil nuts are on top: Size segregation of particulate matter by shaking," *Physical Review Letter*, vol. 58, pp. 1038 – 1040, 1987.

[2] R. Chavez, N. Cheimanoff, and J. Schleifer, "Sampling problems during grain size distribution measurements," *Proceedings of the Fifth International Symposium on Rock Fragmentation by Blasting - FRAGBLAST 5*, pp. 245–252, Aug 1996.

[3] M. J. Thurley, "Three dimensional data analysis for the separation and sizing of rock piles in mining," Ph.D. dissertation, Monash University, December 2002, download from http://image3d6.eng.monash.edu.au/thesis.html.

[4] M. J. Thurley and K. C. Ng, "Identification and sizing of the entirely visible rocks from a 3d surface data segmentation of laboratory rock piles," *Computer Vision and Image Understanding*, vol. 111, no. 2, pp. 170–178, Aug. 2008.

[5] T. Andersson, M. Thurley, and O. Marklund, "Visibility classification of pellets in piles for sizing without overlapped particle error," *Proceedings of the 9th Biennial Conference of the Australian Pattern Recognition Society on Digital Image Computing Techniques and Applications (DICTA 2007)*, pp. 508 – 514, Dec. 2007.

[6] T. Andersson and M. Thurley, "Visibility classification of rocks in piles," *Proceedings of the Conference of the Australian Pattern Recognition Society on Digital Image Computing Techniques and Applications (DICTA 2008)*, pp. 207 – 213, Dec. 2008.

[7] W. Wang, "Image analysis of particles by modified ferret method - best-fit rectangle," *Powder Technolgy*, vol. 165, no. 1, pp. 1–10, Jun 2006.

[8] O. Carlsson and L. Nyberg, "A method for estimation of fragment size distribution with automatic image processing," *Proceedings of the First International Symposium on Rock Fragmentation by Blasting (FRAGBLAST)*, vol. 1, pp. 333 – 345, Aug. 1983.

[9] G. Potts and F. Ouchterlony, "The capacity of image analysis to measure fragmentation, an evaluation using split desktop®," Swebrec - Swedish Blasting Research Centre, Swebrec Report 2, 2005, ISSN: 1653-5006.

[10] M. J. Thurley, "Automated online measurement of particle size distribution using 3d range data," *IFACMMM 2009 Workshop on Automation in Mining, Mineral and Metal Industry*, Oct. 2009.

[11] M. J. Noy, "The latest in on-line fragmentation measurement - stereo imaging over a conveyor," *Proceedings of the Eighth International Symposium on Rock Fragmentation by Blasting - FRAGBLAST*, vol. 8, pp. 61 – 66, Feb. 2006.

[12] D. E. Johnson, *Applied Multivariate Methods for Data Analysts*. Duxbury Press, 1998, iSBN: 0-534-23796-7.

[13] M. J. Thurley and T. Andersson, "An industrial 3d vision system for size measurement of iron ore green pellets using morphological image segmentation," *Minerals Engineering Journal*, vol. 21, no. 5, pp. 405 – 415, 2008.

[14] E. R. Dougherty and R. A. Lotufo, *Hands-On Morphological Image Processing*. SPIE – The International Society for Optical Engineering, 2003, vol. TT59.

[15] R. McGill, J. W. Tukey, and W. A. Larsen, "Variations of box plots," *The American Statistician*, vol. 32, no. 1, pp. 12 – 16, Feb. 1978.

[16] R. O. Duda, P. E. Hart, and D. G. Stork, *Pattern classification*, 2nd ed. Wiley, 2001, iSBN: 0-471-05669-3.

[17] S. J. Press and S. Wilson, "Choosing between logistic regression and discriminant analysis," *Journal of the American Statistical Association*, vol. 73, no. 364, pp. 699 – 705, Dec. 1978.

Paper G

A Machine Vision System for Estimation of Size Distributions by Weight of Limestone Particles During Ship Loading

Authors:
Tobias Andersson, Matthew J. Thurley and Johan E. Carlson

Reformatted version of paper submitted to:
Minerals Engineering, 2010

A Machine Vision System for Estimation of Size Distributions by Weight of Limestone Particles During Ship Loading

Tobias Andersson, Matthew J. Thurley and Johan E. Carlson

Abstract

The size distribution as a function of weight of particles is an important measure of product quality in the mining and aggregates industries. When using manual sampling and sieving, the weight of particles is readily available. However, when using a machine vision system, the particle size distributions are determined as a function of the number of particles. In this paper we first show that there can be a significant weight-transformation error when transforming from one type of size distribution to another. We also show how the problem can be overcome by training a classifier and scaling the results according to calibrated average weights of rocks. The performance of the algorithm is demonstrated with results of measurements of limestone particles on conveyor belts.

1 Introduction

In the aggregates and mining industries suppliers of particulate material, such as crushed rock and palletized iron ore, produce material where the particle size is a key differentiating factor in the quality of the material. Material is classified by size using sieving or screening to produce various products, such as crushed limestone in the sieve-size ranges of 20–40, 40–70 and 60–90 mm. The final products are stored at different locations at the production area until they are loaded onto ships and delivered to buyers.

Suppliers are paid to deliver rocks of particular sizes that buyers can use. For quality control, manual sampling and sieving of rocks that are loaded is conducted. Manual sampling and sieving techniques is the industry standard, and the size distribution of particles is presented as a cumulative percentage by weight for different size classes. The manual sampling and sieving techniques can have long response times (even up to 48 hours), is performed infrequently, and may be inconsistent because of mechanical faults in sieving frames or variation in handling of the analysis equipment by different personnel. Sampling, sieving, and material handling times coupled with delays between steps make manual sampling and sieving unsuitable for efficient quality control of the particles being transported on the conveyor belt.

Image analysis techniques promise a non-invasive, frequent and consistent solution for determining the size distribution of particles in a pile and would be suitable for on-line quality control that enables efficient process control. Such techniques capture information

about the surface of the pile which is then used to infer the particle size distribution.

However, the implementation of an imaging system that is accurate and robust is not a trivial task. Assuming there exists a robust and accurate surface data capturing system with insignificant errors, there are still a number of sources of error relevant to surface analysis techniques that need to be addressed:

- Segregation and grouping errors, more generally known as the "Brazil-nut effect" [1]. These errors arise from the tendency of the pile to separate into groups of similarly sized particles. This is caused by vibration or motion (e.g. as rocks are transported by truck or on a conveyor belt), where large particles tend to move to the surface.

- Capturing errors [2],[3, Ch. 4] caused by the varying probability of a particle to appear on the surface of the pile based on its size.

- Profile errors originate from the fact that only one side of an entirely visible particle can be seen, which may bias the estimation of particle size.

- Overlapping-particle errors [4] are due to the fact that many particles are only partially visible, which results in a large bias toward the smaller size classes if they are treated as small, entirely visible particles.

- Weight-transformation errors occur when the weight of particles in a specific sieve-size class varies significantly. As a sieve-size class is defined by the upper and lower boundaries at which particles pass, elongated particles may have significantly larger volumes than more spherical particles. This error is relevant when using machine vision as transformation from number of particles in specific sieve-size classes to weight of particles is necessary to estimate the size distribution based on weight of particles.

The long-term objective of this research is to develop techniques for efficient quality control by estimating the particle size distribution based on machine vision. Thus, the abovementioned sources of errors need to be addressed to minimize the overall estimation error.

We have previously shown that visibility classification can be used in order to overcome the overlapped particle error [5, 6], by identifying and excluding any partially visible particles prior to size estimation. This is made possible with classification algorithms that use a 3D visibility measure, as proposed by Thurley and Ng [4].

The profile error is considered to be insignificant when using the best-fit rectangle measure to estimate the size of non-overlapped particles [7]. We have previously used the best-fit rectangle to estimate the size distribution of iron ore pellets [8], to enable product identification/classification [9], and to estimate the size distribution [10] of crushed limestone.

Finally we note that capturing errors and the segregation and grouping errors are present in this application and that more research is necessary to fully understand how to minimize these. This is, however, not considered in this paper.

The focus of this paper is to:

- Show how the product identification method presented in [9] can be used to extend and improve the estimation of particle size distribution (by weight of particles) previously presented in [10].
- Show the existence of the weight-transformation error.
- Demonstrate how particle size distributions by number of particles can be converted to a size distribution by weight, given that the type of product has been identified.

The remainder of the paper is organized as follows. Section 2 gives a description of the measurement system. How manual and imaging samples are collected during the measurement campaign is described in section 3. The existence of the weight-transformation error is identified in section 4, along with a proposed strategy for reducing it. Details on how the machine vision system is trained and validated are given in sections 5 and 6.

2 Measurement setup

We use an industrial measurement system based on active triangulation to capture 3D surface data of the flow of rock material on a conveyor belt. The system consists of a laser with line-generating optics and one camera mounted at an angle of approximately 24 degrees between the camera line of sight and the laser line. The system collects images, extracts the laser line, converts the images into 3D surface data, and performs analysis of the captured 3D surface data. An illustration of the imaging system is shown in Figure 1.

Also, a pulse encoder is mounted to the conveyor belt to synchronize the camera to capture 3D profiles of the laser line for every 1 mm movement of the conveyor belt. The data captured with this technique are highly accurate and provides high density 3D point data. Analysis of the data involves segmenting the 3D surface data to identify each rock fragment on the surface of the pile, identifying the non-overlapped particles by visibility classification, and estimating the size of each rock. For a complete description of these steps, see the work by Thurley [10]. The computational speed of the collection of data, conversion to 3D surface data, and analysis of data allows samples to be taken at intervals of approximately 30 seconds.

3 Measurement campaign

A measurement campaign was conducted at Nordkalk's limestone quarry in Storugns during three days when two ships were loaded with three different products. Typically, each ship is loaded with one of the products. During the measurement campaign one larger ship was loaded with two different products, specifically 40–70 and 60–90 mm. In addition, a smaller ship was loaded with the product 20–40 mm. The loading of rocks began on day one with the product 60–90 mm and at 15:22 the product being loaded was changed to 40–70 mm. During day 2 only the 40–70 mm product was loaded and

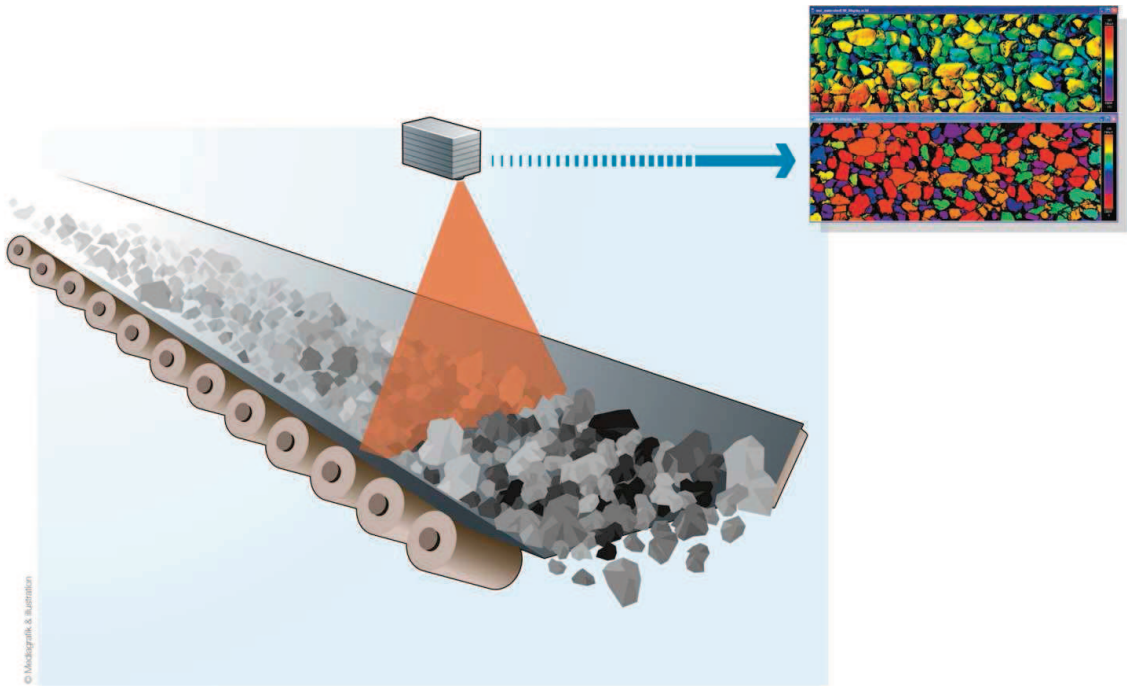

Figure 1: Conceptual image of the imaging system that captures 3D surface data.

Table 1: Loading scheme of ships during the measurement campaign spanning over 3 days.

Day	Loading time	Product (mm)	Manual samples	Imaging samples
1	07:00 - 15:22	60–90	4	345
1	16:30 - 19:00	40–70	2	174
2	07:00 - 15:00	40–70	5	561
3	08:00 - 15:00	20–40	4	469

the first ship departed. The smaller ship was then loaded with the 20–40 mm product during day 3. The loading scheme is summarized in Table 1.

During the loading, samples were extracted for off-line analysis. The samples were divided into a training set consisting of three manual samples of each product and a hold out set, used to validate the proposed techniques using the *hold out method*, as described in [11, p. 220]. The training set was used to investigate the presence of a significant weight-transformation error. Furthermore, one of the three samples of each product in the training set was studied in detail to enable using statistical analysis of variance (ANOVA) [12]. The training set was also used to develop techniques for automated estimation of particle size distributions.

The time when manual samples was collected was also logged in order to allow extraction of imaging data corresponding to each of the manual samples.

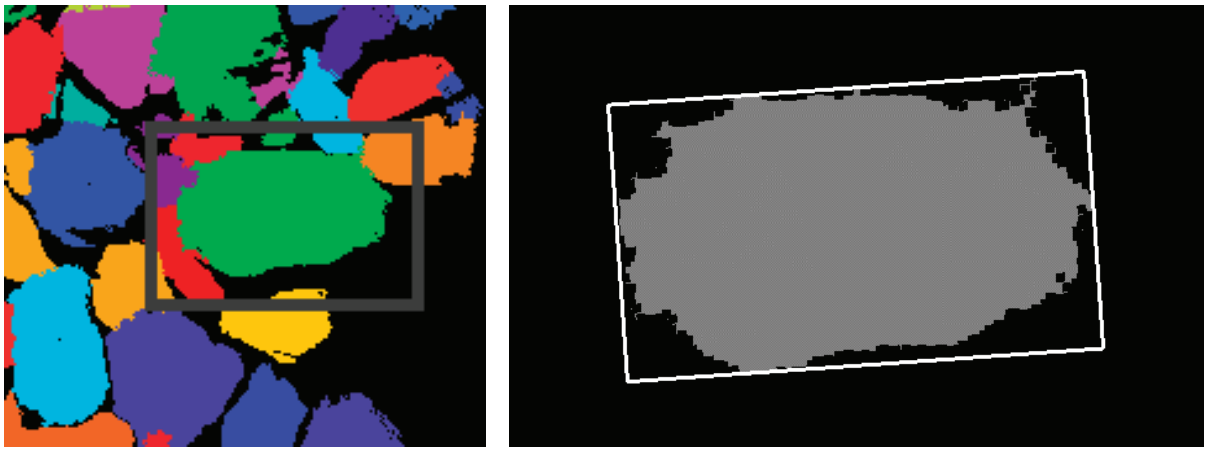

(a) Identified non-overlapped rock (b) Calkulated best-fit rectangle

Figure 2: Identified non-overlapped rock (a) and calculated best-fit rectangle (b).

3.1 Collecting manual samples

The conveyor belt that transports rocks to ships was equipped with a balance to monitor the amount of rocks that have been loaded. During normal production this was used to trigger an automatic sampling machine to collect three manual samples for every product being loaded. The manual samples were later analyzed in the laboratory to estimate the size distribution and chemical composition of the material. During the measurement campaign we used the cumulative weight of rocks being loaded to trigger manual samples of rocks to be taken every 1000 tons. This resulted in 4, 7 and 4 manual samples of the 20–40, 40–70 and 60–90 mm products, respectively.

3.2 Collecting imaging samples

At the same time, the image analysis system collected and analyzed 469, 735 and 345 samples, respectively. The image data collection was synchronized such that the images should, to the best extent possible, be of the same samples as those collected for off-line analysis by the manual sampling procedure described above.

For each non-overlapped rock in a sample, the best-fit rectangle measure [7] was calculated. This measure is the rectangle of minimum area that fits around the 2D projection of each region. The 3D surface data contain X, Y and Z data where the Z data contain height information. The height information was used only in the segmentation and visibility classification steps, and not to calculate the best-fit rectangle measure. In Fig. 2(a) a close-up of all regions is shown. The region enclosed by the white rectangle is determined to be a non-overlapped rock and therefore valid for size estimation. Fig. 2(b) shows the 2D projection of the region and the corresponding best-fit rectangle.

The sieve-size class of each non-overlapped rock is then determined according to the classification scheme described in Section 5.1.

Table 2: Number of particles and total weight of rocks by size class

Sieve size	Number of particles			Weight of particles		
	20–40 mm	40–70 mm	60–90 mm	20–40 mm	40–70 mm	60–90 mm
> 100	-	-	-	-	-	-
90–100	-	-	11	-	-	16.0702
75–90	-	4	25	-	2.3693	25.9672
63–75	-	26	6	-	14.2053	4.8364
50–63	-	77	4	-	22.5161	1.1958
45–50	7	35	3	1.0497	6.3218	0.5447
40–45	44	40	1	5.5192	5.8721	0.1438
37.5–40	40	8	-	3.9637	0.9612	-
31.5–37.5	151	10	5	10.7429	0.8521	0.3788
25–31.5	206	13	3	8.5686	0.5800	0.1341
20–25	524	13	6	11.2890	0.2781	0.1087
16–20	291	7	2	3.2401	0.0696	0.0170
12.5–16	204	13	8	1.1052	0.0535	0.0409
10–12.5	97	17	11	0.2457	0.0367	0.0236

4 Analysis of the average weights of rocks

The presence of a weight-transformation error would mean that samples of different products belonging to the same sieve size class would have a different average weight. Since the source of this error is not fully understood, ANOVA was performed in order to determine if this error was statistically significant.

One manual sample of each of the three products was manually analyzed in detail to conduct ANOVA. First, the manual sample was sieved in the laboratory at Nordkalk using all available sieve decks between 10 mm and 100 mm. Then the three samples, with the rocks divided into different sieve-size classes, were transported to Luleå for further analysis. In the laboratory in Luleå, the weight of each rock was measured using a digital balance. Table 2 shows the number of rocks and the total weight at each sieve deck for the three different products.

Using the total number and the total weight of the rocks at each sieve deck an estimate of the average weight per rock was calculated, seen in Fig. 3. The figure shows that the average weight per rock for the three different product is relatively close for sieve decks up to 31.5 mm or 37.5 mm. For sieve decks larger than 31.5 mm, rocks belonging to the 20–40 mm product have an estimated weight per rock that is lower than for the other products. Also, for the 40–70 product, the estimated average weight per rock follows the 60-90 product up to sieve deck 50 mm. However, from sieve deck 63 mm and larger, rocks that come from the 40–70 product weigh less than rocks from the 60–90 product. To conclude, it appears as if rocks in the upper part of a product's size interval weigh less than rocks from other (larger) products.

Fig. 3 only shows information about the average weight per rock and does not take variation in the weight of the rocks into account. If the variance of the weights is analyzed,

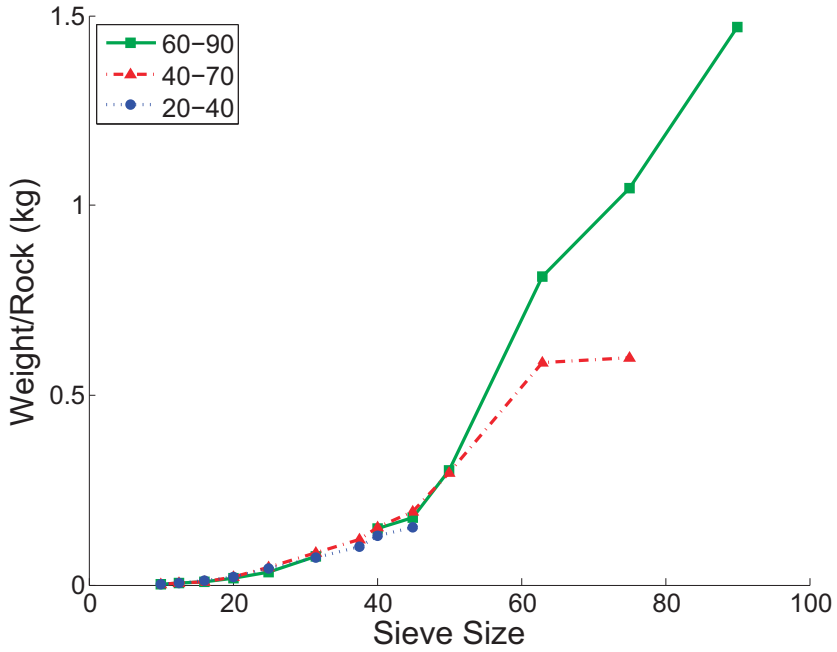

Figure 3: Average weight of rocks for different products.

it is possible to determine if the mean differences are significant. This is done by using ANOVA to test the null hypothesis (H0: all means are equal) against the alternative hypothesis (H1: some means are different) [12]. Table 3 shows the calculated p-values when comparing means between 20–40, 40–70 and 60–90 mm products. Low p-values indicate that we should reject the null hypothesis (all average weights are equal) and conclude that there is in fact a statistically significant difference in average weight for that specific sieve deck. As seen, the p-values are low for sieve decks 31.5 mm and up. This means that there is a significant difference of the average weight of rocks for sieve deck 31.5 mm between the 20–40 mm and 40–70 mm product. We also see that there is a significant difference between the 40–70 mm and the 60–90 mm product for larger sieve decks as the p-value is low for sieve deck 63 and up.

5 Training of the classifier

During the measurement campaign high resolution sieving was performed on the manual samples, registering the weight and number of particles for each size class. The weight was measured using a digital balance and the number of particles was counted by hand. The number of particles for each sample in the training set is shown in Table 4. This training data was used to find decision boundaries that separate the best-fit rectangle values into intervals that correspond to sieve-size classes. Using these decision boundaries, size distributions based on the number of particles can be estimated on new samples acquired by the imaging system.

Table 3: Number and total weight of particles by size class

Sieve size	Average weight of particles (kg)			F_0	$P-$value
	20–40 mm	40–70 mm	60–90 mm		
> 100	-	-	-	-	-
90–100	-	-	1.4609	-	-
75–90	-	0.5923	1.0387	10.6243	0.0030
63–75	-	0.5464	0.8061	10.0198	**0.0035**
50–63	-	0.2924	0.2989	0.0221	0.8823
45–50	0.1500	0.1806	0.1816	3.2871	0.0472
40–45	0.1254	0.1468	0.1438	3.6457	0.0304
37.5–40	0.0991	0.1201	-	6.3744	0.0151
31.5–37.5	0.0711	0.0852	0.0758	2.0793	**0.1283**
25–31.5	0.0416	0.0446	0.0447	0.4823	0.6180
20–25	0.0215	0.0214	0.0181	0.6874	0.5033
16–20	0.0111	0.0099	0.0085	0.8367	0.4341
12.5–16	0.0054	0.0041	0.0051	3.2677	0.0399
10–12.5	0.0025	0.0022	0.0021	2.6054	0.0780

Table 4: Number of particles by size class for training samples

Sieve size	Number of particles								
	20–40 mm			40–70 mm			60–90 mm		
	08 : 39	10 : 51	11 : 52	17 : 20	18 : 11	07 : 46	11 : 00	12 : 48	13 : 53
> 100	-	-	-	-	-	-	1	-	-
90–100	-	-	-	-	-	-	16	9	11
75–90	-	-	-	10	4	2	28	41	25
63–75	-	-	-	27	26	30	9	17	6
50–63	-	1	1	69	77	58	11	4	4
45–50	7	9	6	40	35	68	1	1	3
40–45	44	78	55	33	40	44	3	3	1
37.5–40	40	51	37	8	8	6	3	2	-
31.5–37.5	151	166	167	12	10	33	8	5	5
25–31.5	206	265	263	4	13	20	6	5	3
20–25	524	410	696	11	13	47	37	11	6
16–20	291	92	328	11	7	35	25	3	2
12.5–16	204	67	249	20	13	37	25	12	8
10–12.5	97	29	53	21	17	18	24	24	11

5.1 Finding decision boundaries for sieve-size classification

When all best-fit rectangle areas have been determined from the image data, the task is to find decision boundaries that group these areas into classes that match the sieve-sizes. The same training data set as earlier is used for this.

The problem of determining the decision boundaries must be solved by some numerical optimization technique. In this paper, we used the Nelder and Mead [13] iterative error minimization process. This optimization method is available both in the statistical package R [14] as the function *optim*, or in MATLAB® [15] as the function *fminsearch*. In this work, the MATLAB® version was used. Given an initial estimate of the deci-

sion boundaries the numerical optimization technique will iteratively determine the final boundaries, so that some predefined error function is minimized. Section 5.1 describes the procedure of finding initial decision boundary values, and the error function is described in detail in Section 5.1.

To train a machine vision system to estimate the size distribution accurately, it is important to consider sources of error that affect the overall estimation error. We note that:

- The dynamics of the pile that causes segregation and grouping errors are not known for particles being transported on conveyor belts.

- Chavez et al. [2] proposed a probabilistic model that can be used to correct for the capturing error and Thurley [3, Ch. 4] further improved the modelling of the capturing error when measuring rocks in buckets. However, there is no method available for modeling the capturing error for particles being transported on conveyor belts. Hence, this remains a source of error in this application.

- When performing weight transformation from number of particles to weight of particles, we note that larger particles influence the resulting size distribution more than smaller particles. This is due to the weight difference of particles that can be seen in Table 3 and Figure 3. Thus, to minimize the overall estimation error it is more important to estimate the size of larger particles correctly. Also, the weight transformation should be accurate for the upper part of the size interval of particles being measured.

Finding initial decision boundaries

As all numerical optimization techniques, the Nelder-Mead algorithm requires good initial guesses of the parameters to be estimated, i.e. the decision boundaries for the different sieve-size classes.

From the training data, we first calculate the ideal decision boundaries for each set of sieving data, i.e. the boundaries for the image-based method that would lead to the same partitioning as the manual sieving. This is done separately for each of the three samples for each product. The median values of these are then used as the initial estimates for the Nelder-Mead algorithm.

Based on the observations in the previous section, however, we refine the calculation of the decision boundaries so that undersized particles are ignored. To clarify, we define window functions that are used when calculating the decision boundaries to ignore all particles smaller than a specific sieve-size (S) as seen in Equations 1,2 and 3 for the different products. The reason for this is that larger particles have greater influence on the size distribution, and thus the algorithm should put more emphasis on these particles.

$$Cl_{20-40} = \begin{cases} 1 & \text{if S} \geq 16, \\ 0 & \text{if S} < 16. \end{cases} \tag{1}$$

$$Cl_{40-70} = \begin{cases} 1 & \text{if S} \geq 40, \\ 0 & \text{if S} < 40. \end{cases} \tag{2}$$

$$Cl_{60-90} = \begin{cases} 1 & \text{if S} \geq 75, \\ 0 & \text{if S} < 75. \end{cases} \tag{3}$$

A series of steps are now performed to refine the estimates of the decision boundaries for each product, with the aim of finding good initial guesses of the decision boundaries for the largest particles for each product. The strategy is outlined below:

1. As an initial step, "too small" sieve sizes are considered to be non-visible in the imaging samples and BFR-values below a threshold of $1.5S^2$ are therefore removed from the data. S is set to 16 in this analysis. The threshold was determined experimentally.

2. Using the imaging results (BFR-values) corresponding to the three manual samples of the 20–40 mm product:

   (a) Calculate the ideal decision boundaries for each of the three samples (based on the manual sieving).

   (b) Find the median value of these.

3. Using the imaging results (BFR-values) corresponding to the three manual samples of the 40–70 mm product:

   (a) Use the median decision boundary for sieve size 40 from the 20–40 mm product to discard lower BFR-values.

   (b) Calculate the ideal decision boundaries for each of the three samples (based on the manual sieving).

   (c) Find the median value of these.

4. Using the imaging results (BFR-values) corresponding to the three manual samples of the 60–90 mm product:

   (a) Use the median decision boundary for sieve size 75 from the 40–70 mm product to discard lower BFR-values.

   (b) Calculate the ideal decision boundaries for each of the three samples (based on the manual sieving).

   (c) Find the median value of these.

5. Finally, combine decision boundaries of the three products by using the median decision boundaries calculated for the corresponding sieves, i.e.

   (a) 20–40 mm product: Use sieves up to 40

Table 5: Initial and optimized decision boundaries of best-fit rectangle (mm^2)

Method	Sieve size											
	16	20	25	31.5	37.5	40	45	50	63	75	90	> 100
Initial	384	703	1578	2088	2729	3031	3716	4832	7270	9714	13025	17218
Optimized	409	688	1471	1988	2640	2959	4068	5281	7094	9864	12940	18100

(b) 40–70 mm product: Use sieves from 45 up to 75

(c) 60–90 mm product: Use sieves from 75 and up

These initial decision boundaries are now used as initial guesses in the Nelder-Mead optimization to find decision boundaries that work well for each of the training samples.

Error function

The Nelder-Mead optimization will iteratively update the decision boundaries in order to minimize the error function defined in Equation 4 where the denominator is different for different cases, as seen in Equation 5.

$$\epsilon = \sum_t \left[\sum_x \frac{(C_{x,t} - S_{x,t})^2 Cl_p}{d} \right] \tag{4}$$

$$d = \begin{cases} 1 & \text{if } C_{x,t} = S_{x,t} = 0, \\ C_{x,t} & \text{if } C_{x,t} = 0 \text{ and } S_{x,t} \neq 0, \\ S_{x,t} & \text{if } S_{x,t} = 0 \text{ and } C_{x,t} \neq 0, \\ C_{x,t} S_{x,t} & \text{otherwise.} \end{cases} \tag{5}$$

where $C_{x,t}$ and $S_{x,t}$ are the fractions of particles in sieve-size class x for sample t for the imaging method and the manual sieving, respectively.

The resulting initial and final decision boundaries are shown in Table 5.

5.2 Finding correct weight transformation by product identification

To estimate the size distribution based on the weight of particles, the number of particles in each sieve-size class has to be transformed to weight of particles. As we have just seen that the average weight per rock for a given sieve size differs among the products, the transformation must take this difference into account. The transformation is a simple scaling, where the average weight of rocks in a specific sieve class is multiplied by the number of rocks found using the imaging system. This scaling is determined from the training data set. However, to use the correct scaling the current product type must be known. As shown in [9], the training data can be used to calibrate a classifier that,

Table 6: Number and total weight of particles by size class

Sieve size	Average weight of particles (g)		
	20–40 mm	40–70 mm	60–90 mm
> 100	206	684.2	2016.0
90–100	206	684.2	1148
75–90	206	684.2	979.1
63–75	206	554.2	656.5
50–63	206	300.4	285.1
45–50	172.5	201.1	190.0
40–45	129.6	152.8	143.8
37.5–40	101.9	121.7	121.5
31.5–37.5	72.24	72.60	76.00
25–31.5	42.18	45.46	35.88
20–25	22.20	21.80	20.34
16–20	11.72	10.23	10.17
12.5–16	6.033	4.786	4.822
10–12.5	2.475	2.054	1.814

based on the imaging data, determine which product is present on the conveyor belt. Altogether this means that the size distribution by weight can be estimated following these steps:

1. Use a training data set to calibrate a classifier that determines which product is present, following the steps in [9].

2. Based on the training set, determine the average weight per rock in each sieve size class. The results of this are shown in Table 6.

3. Estimate the sieve-size distribution based on the number of rocks, following the procedure described in Section 5.1.

4. Scale the sieve-size distribution using the average weight per rock determined in 2.

6 Final result

To evaluate the performance of the proposed method, the size distributions by weight were estimated for the three products, using data that were withheld during the training of the classifier. The results are shown in Fig. 4. The solid lines mark the true distributions by weight, which were determined off-line. The dashed lines mark the estimates by the proposed algorithm. As the figure shows, the algorithm performs well, also on data not used in the calibration.

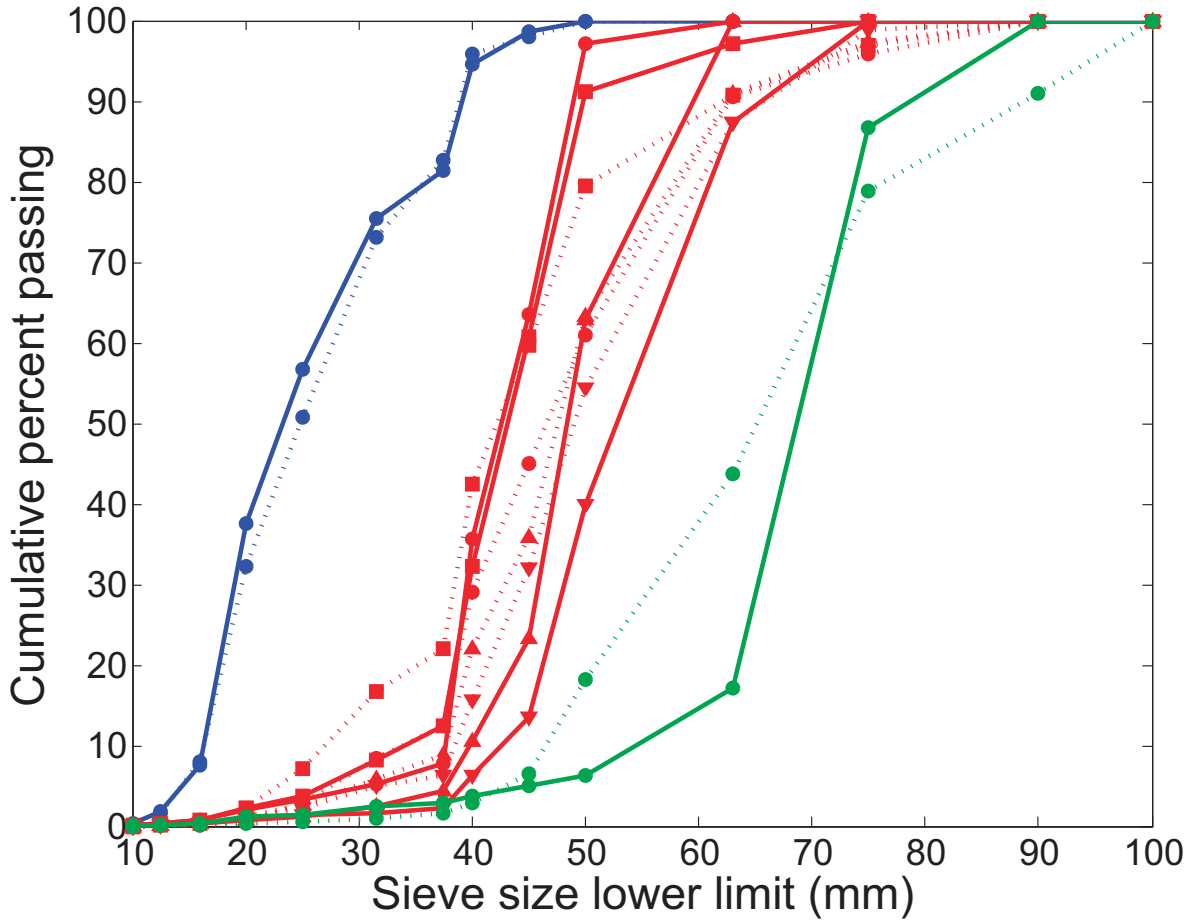

Figure 4: Known (solid line) and estimated (dashed line) size distribution based on weight for validation data.

7 Conclusions

In this paper we proposed a machine vision method for determining the size distribution based on weight, for crushed limestone rocks on conveyor belts. It was also shown that the weight of particles in a certain sieve-size class differ significantly from one product to another, implying that different transformations between the number of particles and the weight of particles must be used. The particle sizes were first estimated by number of particles based on high-resolution 3D imaging data. The transforming function to a size distribution by weight was then determined by calibrating the system based on a small training data set. Results on new data shows that, provided the type of product is known, good estimates of the particle size distribution by weight can be obtained.

8 Acknowledgments

We wish to thank ProcessIT Innovations for all their time and effort in making this research possible. We also want to thank MinBaS II Research program and Nordkalk for their participation and support. We especially say thank you to Madeleine Hägbom and Kajsa Hägbom for helping us with laboratory work at Nordkalk. Finally, we thank our measurement technology partners, MBV Systems. In addition we acknowledge the EU INTERREG IVA Nord program for partially supporting this research.

References

[1] A. Rosato, K. J. Strandburg, F. Prinz, and R. H. Swendsen, "Why the brazil nuts are on top: Size segregation of particulate matter by shaking," *Physical Review Letter*, vol. 58, pp. 1038 – 1040, 1987.

[2] R. Chavez, N. Cheimanoff, and J. Schleifer, "Sampling problems during grain size distribution measurements," *Proceedings of the Fifth International Symposium on Rock Fragmentation by Blasting - FRAGBLAST 5*, pp. 245–252, Aug 1996.

[3] M. J. Thurley, "Three dimensional data analysis for the separation and sizing of rock piles in mining," Ph.D. dissertation, Monash University, December 2002, download from http://image3d6.eng.monash.edu.au/thesis.html.

[4] M. J. Thurley and K. C. Ng, "Identification and sizing of the entirely visible rocks from a 3d surface data segmentation of laboratory rock piles," *Computer Vision and Image Understanding*, vol. 111, no. 2, pp. 170–178, Aug. 2008.

[5] T. Andersson, M. Thurley, and O. Marklund, "Visibility classification of pellets in piles for sizing without overlapped particle error," *Proceedings of the 9th Biennial Conference of the Australian Pattern Recognition Society on Digital Image Computing Techniques and Applications (DICTA 2007)*, pp. 508 – 514, Dec. 2007.

[6] T. Andersson and M. Thurley, "Visibility classification of rocks in piles," *Proceedings of the Conference of the Australian Pattern Recognition Society on Digital Image Computing Techniques and Applications (DICTA 2008)*, pp. 207 – 213, Dec. 2008.

[7] W. Wang, "Image analysis of particles by modified ferret method - best-fit rectangle," *Powder Technolgy*, vol. 165, no. 1, pp. 1–10, Jun 2006.

[8] M. J. Thurley and T. Andersson, "An industrial 3d vision system for size measurement of iron ore green pellets using morphological image segmentation," *Minerals Engineering Journal*, vol. 21, no. 5, pp. 405 – 415, 2008.

[9] T. Andersson, M. J. Thurley, and J. E. Carlson, "On-line product identification during ship loading of limestone based on machine vision," *Machine Vision and Applications*, in submission.

[10] M. J. Thurley, "Automated online measurement of particle size distribution using 3d range data," *IFACMMM 2009 Workshop on Automation in Mining, Mineral and Metal Industry*, Oct. 2009.

[11] D. E. Johnson, *Applied Multivariate Methods for Data Analysts*. Duxbury Press, 1998, iSBN: 0-534-23796-7.

[12] D. C. Montgomery, *Design and Analysis of Experiments*. John Wiley & Sons, 2009, ISBN: 978-0-470-39882-1.

[13] J. Nelder and R. Mead, "A simplex method for function minimisation," *The Computer Journal*, vol. 7, pp. 308–313, 1965.

[14] R. Ihaka and R. Gentleman, "R: A language for data analysis and graphics," *Journal of Computational and Graphical Statistics*, vol. 5, no. 3, pp. 299–314, 1996, http://www.r-project.org/.

[15] The Mathworks, Inc., "MATLAB," *http://www.mathworks.com*, 2010.